Ann Surg Oncol (2014) 21:2097–2104
DOI 10.1245/s10434-013-3444-1

Annals of
SURGICAL ONCOLOGY
OFFICIAL JOURNAL OF THE SOCIETY OF SURGICAL ONCOLOGY

ORIGINAL ARTICLE – TRANSLATIONAL RESEARCH AND BIOMARKERS

Molecular Imaging of Tumor-Associated Angiogenesis Using a Novel Magnetic Resonance Imaging Contrast Agent Targeting $\alpha_v\beta_3$ Integrin

Isabelle Debergh, MD[1], Nancy Van Damme, PhD[1], Dieter De Naeyer, PhD[2], Peter Smeets, MD[3], Pieter Demetter, MD, PhD[4], Philippe Robert, PhD[5], Sabin Carme, PhD[5], Piet Pattyn, MD, PhD[1], and Wim Ceelen, MD, PhD[1]

[1]Department of Surgery, University Hospital, Ghent, Belgium; [2]Department of Biomedical Engineering, IBITECH, Ghent University, Ghent, Belgium; [3]Department of Medical Imaging, Ghent University Hospital, Ghent, Belgium; [4]Department of Pathology, ULB Erasme, Brussels, Belgium; [5]Guerbet Research, Paris, France

ABSTRACT

Background. The recent introduction of biological anticancer therapy has renewed the interest in functional imaging of tumor-associated angiogenesis (TAA) as a tool to monitor early therapy response. The present study evaluated imaging of TAA using P1227, a novel, small molecular magnetic resonance imaging (MRI) probe targeting $\alpha_v\beta_3$ integrin.

Methods. HT29 human colorectal cancers were grown in athymic mice. Dynamic MRI was performed using a three-dimensional VIBE sequence up to 110 min after injection of P1227 or gadolinium–tetraazacyclododecane tetraacetic acid (Gd–DOTA). Specificity was assessed by using P1227 1 h after intravenous administration of the $\alpha_v\beta_3$ inhibitor cilengitide. Regions of interest were drawn encompassing the tumor rim and normal muscle. Imaging data were compared with microvessel density and $\alpha_v\beta_3$ expression.

Results. Using P1227, specific enhancement of the angiogenic tumor rim, but not of normal muscle, was observed, whereas Gd–DOTA enhanced tumor and normal muscle. After administering cilengitide, enhancement with P1227, but not with DOTA, was significantly suppressed during the first 20 min. When using P1227, a significant correlation was observed between normalized enhancement of the tumor rim and immunohistochemical $\alpha_v\beta_3$ integrin expression.

Conclusions. Molecular MRI using a small monogadolinated tracer targeting $\alpha_v\beta_3$ integrin and moderate magnetic field strength holds promise in assessing colorectal TAA.

Early assessment of response to cytotoxic therapy is an area of intense investigation. Indeed, the ability to demonstrate activity early in the course of therapy not only allows to predict an individual patient's prognosis but also to tailor the therapeutic strategy by timely discontinuation of inactive regimens. Moreover, early imaging of tumor response is a valuable tool in preclinical and early phase clinical drug development.

Changes in the physical dimension of a solid tumor, which underly the traditional RECIST criteria, often occur late in the course of therapy.[1] Also, as exemplified by molecular therapy of gastrointestinal stromal tumors, significant tumor response can occur without any accompanying change in tumor dimension.[2] Early iconographic assessment of tumor response is not (only) based upon morphological properties, but on functional properties of the neoplastic tissue. Research for other valuable early imaging biomarkers is currently ongoing. Since the introduction of agents targeting tumor angiogenesis, increasing efforts have been invested in functional imaging of the neoplastic vascular bed. Importantly, it has been shown that the earliest functional change in response to anti-angiogenic therapy is 'microvessel normalization', i.e. the return from a grossly distorted anatomy and function to more physiological microvascular properties.[3] One of the hallmarks of this process is a decrease in microvascular permeability. We recently showed that dynamic contrast-enhanced (DCE) magnetic resonance imaging (MRI) incorporating mathematical modeling allows to quantify

First Received: 7 August 2013;
Published Online: 20 December 2013

W. Ceelen, MD, PhD
e-mail: wim.ceelen@ugent.be

these early changes in microvessel permeability as well as tumor perfusion.[4,5]

Although of interest, these parameters remain indirect estimators of tumor angiogenesis. Direct, specific imaging requires probes directed against moieties expressed on the proliferating endothelial cell (EC) surface. A potential target is $\alpha_v\beta_3$ integrin, which is selectively expressed on activated EC during migration through the basement membrane in the angiogenic process.[6,7] This protein is not upregulated on quiescent EC.[8] Here, we studied a novel $\alpha_v\beta_3$ integrin-directed molecular MRI tracer (P1227) as a tool to visualize tumor angiogenesis in a colorectal xenograft model.

METHODS

Animals and Tumor Model

Colorectal cancer xenografts (HT29) were subcutaneously grown in the hind leg of nude mice (athymic nu/nu, Harlan Laboratories, The Netherlands). Animals were housed separately in plastic cages with free access to tap water and standard pellet food. When tumors reached a size of 0.2–0.3 cm^3 (after 8–10 days), MRI imaging was performed. The protocol was approved by the local Animal Research Institutional Review Board.

MR Imaging Protocol

Dynamic MR image acquisition was performed on a MAGNETOM Symphony 1.5 T clinical scanner (Siemens Healthcare, Brussels, Belgium) using a wrist coil (diameter 10 cm). Imaging was performed using a T1-weighted 3D VIBE sequence (FOV 180 × 80, matrix size 384 × 384, voxel dimension 0.5 × 0.5 × 2 mm^3, repetition time/echo time 6.78/2.78 ms, flip angle 12°, 60 slices, total duration per scan 9 min 25 s). Images were acquired at baseline (before contrast injection) and at regular intervals up to 225 min post-injection. At each timepoint, 60 images were acquired.

Signal intensity (SI) was measured in blinded, manually drawn regions of interest (ROIs) encompassing the tumor rim (outer third of the tumor volume) and normal tissue (contralateral paravertebral muscle). Normalized enhancement ratio (NER) was calculated as the ratio of enhancement in the tumor rim over enhancement in normal muscle tissue.

MR Contrast Agent

The contrast agent (CA) (P1227, Guerbet Research, Paris, France) is a tetraazacyclododecane tetraacetic acid (DOTA)–gadolinium (Gd) chelate linked to a cyclic arginyl-glycyl-aspartic acid (RGD) peptide (molecular weight [MW] = 1297 Da). The MW of Gd–DOTA is 560 Da. The r1 relaxivities of P1227 and Gd–DOTA in plasma at 37 °C and 1.5 T are 8.3 mM^{-1} s^{-1} and 3.8 mM^{-1} s^{-1}, respectively. The binding half maximal inhibitory concentration of P1227, as tested with enzyme-linked immunosorbent assay (ELISA) on purified protein, is 3 nM.

Four experimental groups were studied. In the first group, imaging was performed before and after injection of P1227 (dose 50 μmol Gd/kg) [$n = 15$], while in the second (control) group mice underwent imaging before and after injection of Gd–DOTA (Dotarem®, Guerbet, Paris, France; dose 100 μmol Gd/kg) [$n = 9$]. The choice of doubling the Gd–DOTA dose was based on the much higher relaxivity of P1227. In the third and fourth groups, imaging with P1227 ($n = 9$) or Gd–DOTA ($n = 6$), respectively, was performed 1 h after intravenous administration of the $\alpha_v\beta_3$ inhibitor cilengitide (dose 1800 mg/m^2, Merck KGaA, Darmstadt, Germany). All products were injected as a rapid intravenous bolus through the tail vein.

Immunohistochemistry

On the day after MR imaging, tumors were excised and all mice were sacrificed using cervical dislocation. Half of the tumor tissue was fixed in 10 % formalin, embedded in paraffin, and 4 μm thick sections were cut and mounted for immunohistochemistry. Factor VIII [von Willebrand factor (vWF), FVIII] immunostaining was used to visualize tumor microvessels and to calculate microvessel density (MVD). FVIII staining and MVD calculation were performed as described earlier.[9] The other half of the tumor was snap frozen in liquid nitrogen, cut in 5 μm-thick sections and mounted for immunohistochemistry with mouse anti-human integrin $\alpha_v\beta_3$ (US Biological—Immunosource), similar to the procedure of Schnell et al.[10]

Western Blot Analysis

Quantification of $\alpha_v\beta_3$ integrin protein expression using western blot, was performed as described by Schnell et al.[10] Briefly, snap-frozen tumor tissues were lysed in radioimmunoprecipitation assay buffer by sonication. Total protein content was determined with the Bio-Rad DC protein assay kit (Bio-Rad, Nazareth, Belgium). 50 μg of protein per lane was mixed with LDS sample buffer (NuPAGE®, Invitrogen, Merelbeke, Belgium). The proteins were denatured by heating at 70 °C for 10 min, separated with 170 V over 1 h in running buffer (NuPAGE® MES, Invitrogen). After that, proteins were transferred to a nitrocellulose membrane (GE Healthcare, Buckinghamshire, UK) by a semidry blotting technique. Next, membranes were blocked over 1 h at room temperature. The primary antibodies against integrin subunits (polyclonal rabbit anti-integrin α_v subunit AB1930, dilution 1:5000; and polyclonal rabbit anti-integrin β_3

subunit AB1932, dilution 1:2,000; Chemicon, Millipore, MA, USA) were incubated overnight at 4 °C. Bound antibodies were labeled using a secondary antibody coupled to alkaline phosphatase (1:2,000 goat anti-rabbit immunoglobulin) for 1 h. Visualization was performed using chromogen nitroblue tetrazolium salt and 5-bromo-4-chloro-3-indolyl phosphate (BCIP/NBT substrate kit, Invitrogen). Blots were subsequently stripped and reprobed with monoclonal antibody against β-tubulin (Abcam, Cambridge, UK; dilution 1:5,000) as an internal control for protein loading. All blots were digitized by scanning, mean intensity of each different chain was measured with National Institutes of Health Image J software and the overall relative intensity of the different chains of interest was calculated (mean intensity of chain of interest/mean intensity of tubulin).

Statistical Analysis

Data are expressed as mean ± standard error of the mean, or median (interquartile range). Differences were analyzed using the Student *t* test or Mann–Whitney rank sum test where appropriate. Correlations between histology data and imaging parameters were assessed with Spearman's rank correlation. Statistical analysis was performed with SigmaStat 11.0 (Systat Software, Richmond, CA, USA). Results were considered statistically significant when the probability of a type I error was ≤5 %.

RESULTS

Signal Enhancement in Tumor and Normal Muscle After Injection of P1227 Versus Gadolinium–Tetraazacyclododecane Tetraacetic Acid

Typical enhancement patterns are illustrated in Fig. 1. It may be appreciated that, as illustrated by the SI histograms, P1227 specifically enhanced the angiogenic tumor rim while Gd–DOTA was more homogeneously distributed towards the center of the tumor. Quantitative evaluation of the SI changes observed in the tumor rim, entire tumor, and normal muscle is provided in Fig. 2, where NER are depicted. NER in the entire tumor appears to be lower than NER in the tumor rim at each timepoint. When using P1227, significant enhancement of SI was observed of the tumor rim (569 ± 15 vs. 472 ± 21; $p = 0.004$; *t* test) but not of normal muscle. However, when using Gd–DOTA, significant enhancement of SI was noted in both tumor tissue and normal tissue (614 ± 24 vs. 430 ± 17 in muscle tissue; $p < 0.001$; *t* test). For both CAs, a peak in normalized enhancement was observed after 5 min. When using P1227, normalized enhancement after 225 min did return to baseline. When using Gd–DOTA, however, normalized enhancement at 225 min remained significantly elevated compared with baseline (precontrast) level (1,261 ± 0,0818 vs. 1,098 ± 0,122; $p = 0.035$; *t* test).

Signal Enhancement in the Tumor Rim with and without Pretreatment with Cilengitide

To verify whether P1227 binds the target integrin in a specific way, the inhibitor cilengitide was administered 1 h before imaging with P1227 ($n = 9$). The results, expressed as the ratio of enhancement in the tumor rim over enhancement in normal tissue, are illustrated in Fig. 3. Administration of cilengitide before P1227 resulted in a significantly lower normalized contrast enhancement of the tumor rim during the first 20 min ($p = 0.027$; *U* test). Between 35 and 60 min, NER was still higher in the P1227 group, but without showing statistically significant differences compared with the cilengitide pretreated group. After 80–90 min, however, no differences in SI were observed between both groups. When DOTA was used, however, pretreatment with cilengitide did not affect tumor rim enhancement.

Immunohistochemistry and Western Blot

MVD (vWF staining) in all tumors, expressed as the vascular area fraction, was significantly higher in the tumor rim compared with the entire tumor [11.25 % (8.7–16.7) vs. 8.4 % (4.6–12.2); $p < 0.001$; *U* test). Also, the percentage of $\alpha_v\beta_3$ integrin-expressing endothelium was 12.8 % (10.9–16.9) in the tumor rim versus 11.2 % (7.9–14.6) in the entire tumor ($p = 0.002$; *U* test; Fig. 4b, c). The results of western blotting confirmed that protein expression of the α_v and β_3 subunit was significantly higher in the vascular tumor rim (Fig. 4a, d). Three different molecular masses can be found in α_v subunits (at 137 kDa and, to a much lesser extent, at 27 and 25 kDa) and in β_3 subunits (between 90 and 100 kDa, and degradation products at 64 and 52 kDa).[10]

Correlation of MRI Parameters with Histology Data

Correlation data are summarized in Table 1. When using Gd–DOTA, no correlation was observed between the NER in the tumor rim and either $\alpha_v\beta_3$ integrin expression or MVD. However, when using P1227, a statistically significant positive correlation was observed between $\alpha_v\beta_3$ integrin expression and the NER at 35, 50, and 65 min post-contrast injection.

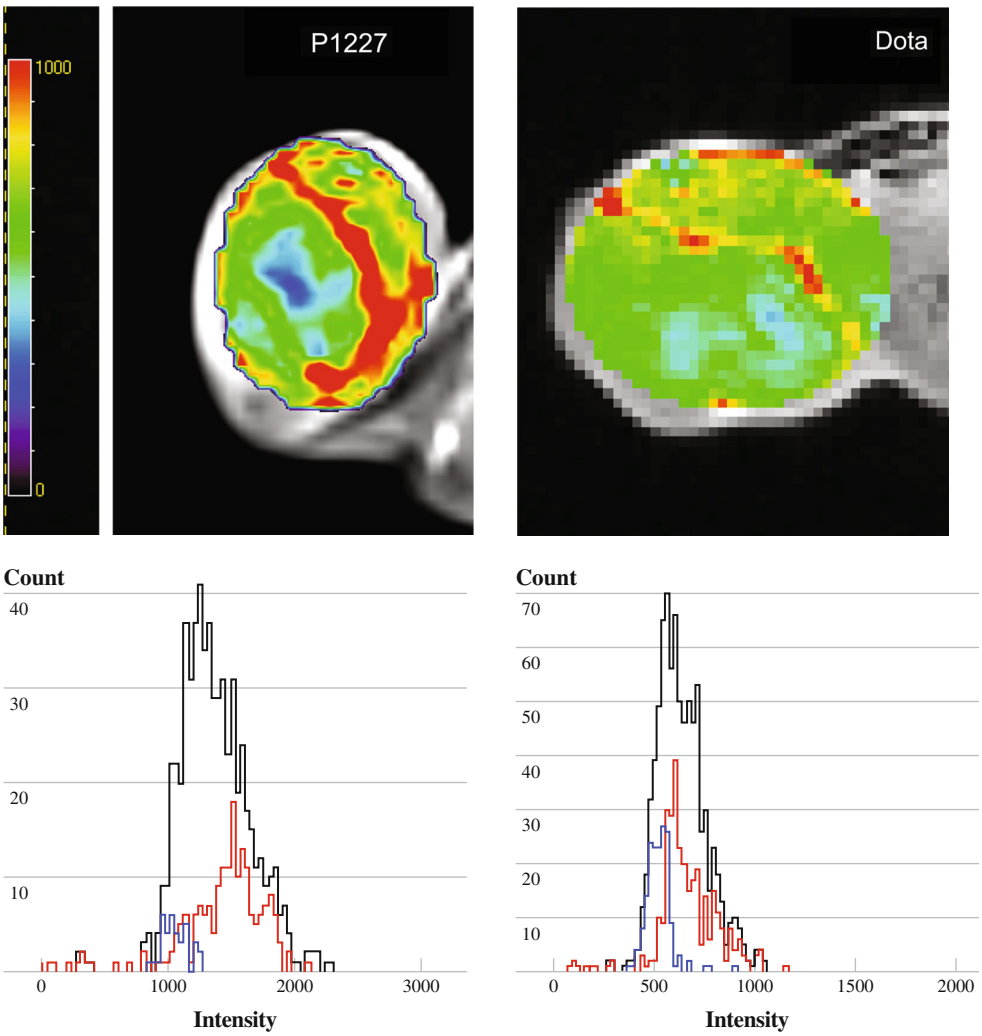

FIG. 1 Enhancement pattern observed following administration of P1227 (*upper left*) or gadolinium–tetraazacyclododecane tetraacetic acid (*upper right*). The *histograms* (*lower row*) show frequency of signal intensities in the entire tumor (*black*), central (*core*) region (*blue*), and tumor rim (*red*)

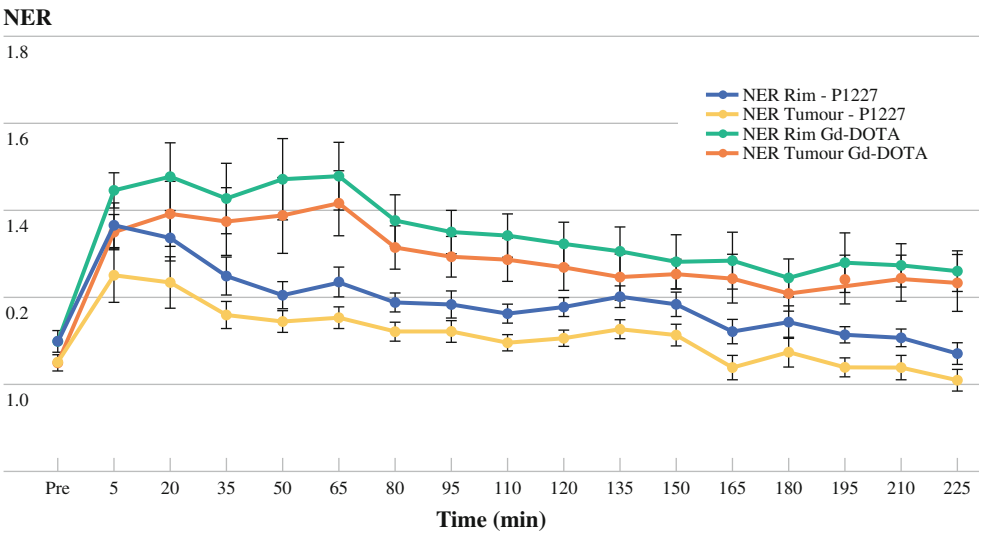

FIG. 2 NER over time in regions of interest encompassing the tumor rim and entire tumor following administration of P1227 or Gd–DOTA. *Bars* standard error of the mean. *NER* normalized enhanced ratio, *Gd–DOTA* gadolinium–tetraazacyclododecane tetraacetic acid

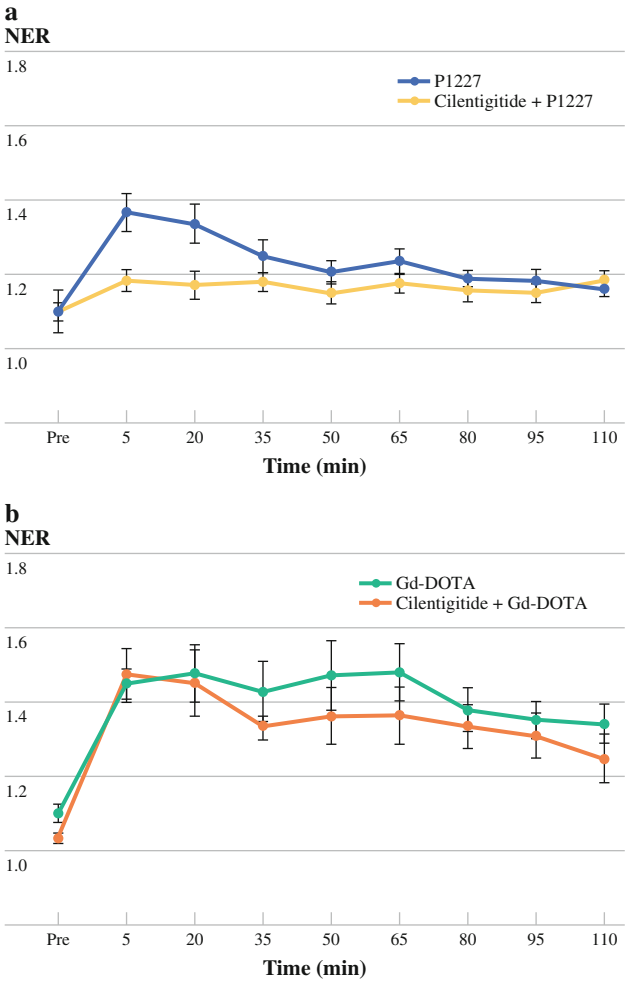

FIG. 3 NER of the tumor rim over time following administration of DOTA or P1227 with or without pretreatment with cilengitide. *Bars* standard error of the mean. *NER* normalized enhanced ratio, *Gd–DOTA* gadolinium-tetraazacyclododecane tetraacetic acid

DISCUSSION

We have studied the feasibility to probe tumor angiogenesis using a novel MR CA targeting $\alpha_v\beta_3$ integrin. The integrins are a group of evolutionary conserved heterodimeric cell surface receptors which are essential in cell-cell and cell-matrix interactions.[11] Some subtypes are highly overexpressed on cancer cells: $\alpha_v\beta_3$, $\alpha_v\beta_5$, and $\alpha_5\beta_1$ play an important role in mediating tumor angiogenesis, while $\alpha_v\beta_6$ and $\alpha_6\beta_4$ have pivotal functions in cell migration and metastasis.[12,13] These interesting properties and their high level of expression on some tumor types, make the integrins ideal candidates for targeted therapy and imaging studies. More specifically, integrin $\alpha_v\beta_3$ is overexpressed by some tumor cell types (colorectal cancer, lung cancer, ovarian cancer, breast cancer, glioblastoma multiforme), and by most tumor-associated ECs, but not by normal blood vessels.[13] Inhibitory peptides and anti-integrin monoclonal antibodies are currently being investigated in solid tumors, with early evidence suggesting clinical benefit in the use of an anti-$\alpha_v\beta_3$ antibody in colorectal cancer, renal cell carcinoma, and melanoma. The recognition sequence of the $\alpha_v\beta_3$ integrin is the RGD peptide on the β_3 domain, and its most abundant ligands are components of the extracellular matrix such as fibronectin, vitronectin, and fibrinogen.[14] Expression of integrin $\alpha_v\beta_3$ by ECs is stimulated by angiogenic growth factors such as basic fibroblast growth factor, tumor necrosis factor-α and interleukin-8, and is upregulated not only in neoplastic tissue but also during wound healing and inflammation.[8] The HT29 colorectal cancer cell line used in the present experiment was shown to express integrins $\alpha_v\beta_5$, $\alpha_v\beta_6$, and $\alpha_v\beta_8$.[15,16] The expression of human integrin $\alpha_v\beta_3$ is negligible on HT29 tumor cells, but tumors express murine integrin $\alpha_v\beta_3$, which is present on newly formed tumor vasculature in this mouse model. Recently, several studies proved, with the HT29 model, the relation between RGD-based radiotracer uptake in tumors and the expression levels of both human integrin $\alpha_v\beta_3$ and murine integrin $\alpha_v\beta_3$.[17,18] In our study, the HT29 model allowed us to focus directly on tumor-associated angiogenesis (TAA) via this novel $\alpha_v\beta_3$ integrin-specific molecular tracer (P1227).

The utility of MRI-based molecular imaging is hampered by its low sensitivity to visualize epitopes, which are often present in the nanomolar range. Therefore, efforts have been directed towards the combination of the target-specific molecule with a large (super)paramagnetic payload. Several authors have used RGD-coupled liposomes containing Gd–DTPA to visualize tumor angiogenesis.[19,20] Others have used RGD-labeled ultrasmall superparamagnetic iron oxide nanoparticles (USPIO) and T2-weighted imaging.[21–23] Several disadvantages are associated with the use of these large carriers. First, since they are exclusively limited to the vascular compartment, binding sites on the tumor cells and extracellular matrix will be out of reach.[24] Second, endocytosis of the Gd-labeled liposomes may lead to 'quenching' of the MRI signal. Third, concerns have risen regarding the safety and biological side effects of USPIOs in early clinical trials, although these were usually mild and reversible.[25] Finally, the pharmacokinetic properties of nano-sized tracers, including a plasma half-life of several hours and retention by the reticuloendothelial system better suit therapeutic than diagnostic purposes.

Here, we report for the first time the use of a low MW tracer (1297 Da, diameter of 1–2 nm) consisting of a routinely used monogadolinated CA linked to an RGD peptide as a tool to image TAA. The results demonstrate that, compared with non-targeted DOTA (MW = 558 Da), P1227 better discriminates angiogenic tumor tissue from normal muscle. Gd–DOTA pools immediately in the blood, as both SI in the tumor rim and muscle are high, whereas

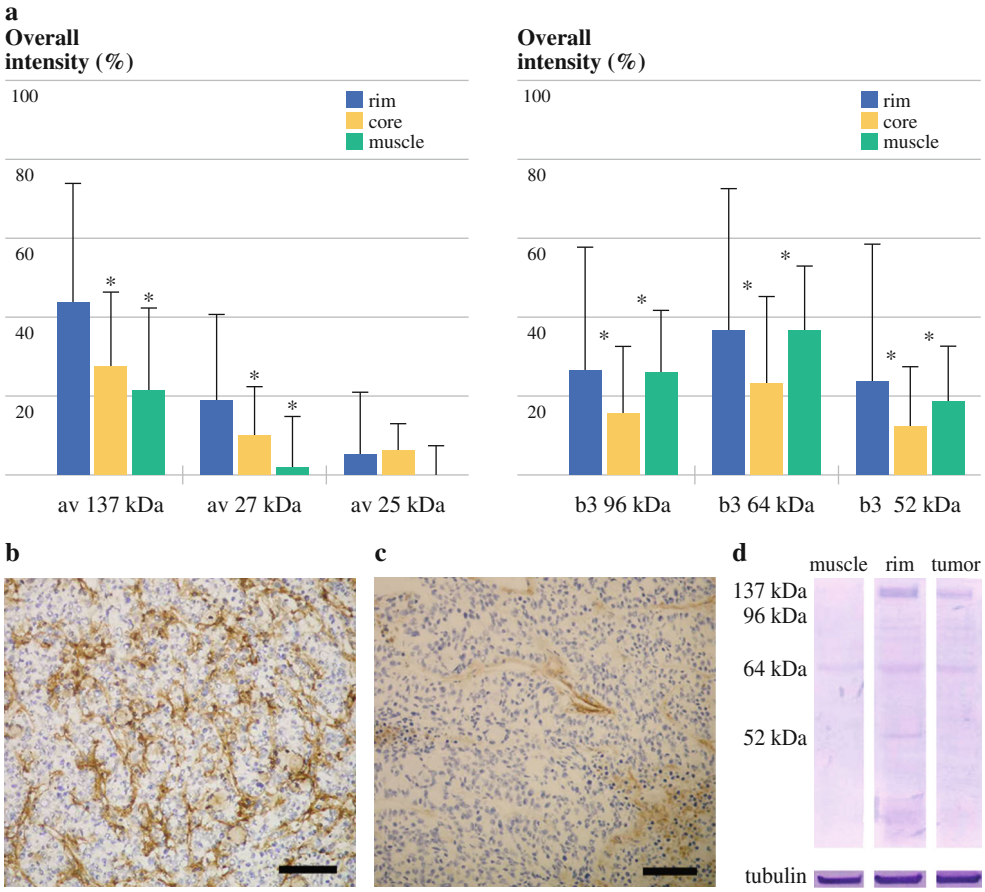

FIG. 4 Protein expression measured by western blot of αv chains and β3 chains (**a**, **d**). *Bars* standard deviation. Representative $\alpha_v\beta_3$ integrin immunohistology of the tumor rim (**b**) and tumor center (**c**). *Scale bar* 100 μm. * $p \leq 0.05$

TABLE 1 Correlation between histology and imaging parameters (normalized enhancement ratio of the tumor rim)

	5 min	20 min	35 min	50 min	65 min	80 min
$\alpha_v\beta_3$ integrin						
DOTA	0.7	0.92	0.88	0.36	0.72	0.06
P1227	0.43	0.39	0.019	0.0092	0.046	0.35
Microvessel density						
DOTA	0.52	0.63	0.99	0.9	0.59	0.86
P1227	0.44	0.69	0.57	0.49	0.67	0.47

Numbers indicate *p* values from Pearson correlation analysis

DOTA tetraazacyclododecane tetraacetic acid

P1227 does not change SI in muscle. Furthermore, aspecific accumulation of Gd–DOTA in the well vascularized oedemateous tumor tissue leads to persistent high NERs, even after 225 min. At this point, SI in normal muscle tissue did return to baseline, indicating that the high SI of the tumor rim is due to extravasated Gd–DOTA tracer. This may be explained by the higher MW of P1227, which limits diffusion across normal and leaking tumoral microvessel linings. Retention of the tracer due to specific binding to the target integrin was demonstrated by the near complete disappearance of P1227-induced tumor enhancement after pretreatment with cilengitide. Cilengitide is a known inhibitor of the integrins $\alpha_v\beta_3$, $\alpha_v\beta_5$, and $\alpha_5\beta_1$, but blocking the other integrins is not interfering with the imaging result of HT29 tumors as P1227 was designed to have only specificity for the RGD sequence on the β_3 domain of the $\alpha_v\beta_3$ integrin. Compared with nanoparticle imaging, the peak in signal enhancement after injecting P1227 occurs much earlier (after 5 min). Sipkins et al.,[26] who used an $\alpha_v\beta_3$-targeting antibody conjugated paramagnetic liposome to image tumor angiogenesis in a rabbit model, noted specific enhancement of angiogenic areas after a time window of 24 h. Similarly, Winter et al.,[19] who used an integrin-directed nanoparticle with a size of ~70 nm, observed steadily increasing SI in the experimental tumor model until the completion of the imaging after 120 min. The relatively low accumulation of the tracer in the present model may be explained by the smaller size of the agent and by low internalization by HT29 cells, as demonstrated in vitro by Bloch et al.[27] This HT29 tumor cell line, is known to express little amounts of integrin

$\alpha_v\beta_3$.[15] Radiolabeled cyclic RGD peptides specifically accumulate in $\alpha_v\beta_3$-expressing tumors by higher probe internalization, and increases when cyclic peptides are polymerized.[28,29]

The specificity of the novel tracer for $\alpha_v\beta_3$ integrin was further demonstrated by the correlation between immunohistochemical staining and the observed MRI enhancement. No statistically significant correlation was noted with MVD, yet the Factor VIII staining method used does not allow to distinguish proliferating, active ECs from resting microvessel linings.

Several limitations apply to the interpretation of the present results. First, although immunohistochemistry of integrin chain expression can be regarded as a valid surrogate marker of active angiogenesis, no golden standard is available at present. Correlation of MR imaging with in vivo microscopic imaging of fluorescently-labelled tracers may hold promise in this regard.[30] Second, although expression of $\alpha_v\beta_3$ integrin is generally low in healthy tissue, it is known to be expressed by several other cell types (epithelial cells, fibroblasts, smooth muscle cells) and to be implicated in other conditions, including arterial stenosis.[31] An additional tumor model with different integrin expression level to demonstrate the ability of the probe would be interesting to discriminate tissues with different expression levels. Also, although the human HT29 is commonly used in colorectal cancer research, the representativeness of a xenograft model for the clinical situation remains partly uncertain. Finally, it may be envisaged that compared with nanoparticles with a high Gd payload, the sensitivity of the current tracer for detecting small lesions is limited. This may also explain the fact that we did not find a significant correlation between imaging parameters and MVD.

CONCLUSIONS

We have shown that molecular MRI using a small monogadolinated tracer targeting $\alpha_v\beta_3$ integrin holds promise in safely and non-invasively assessing colorectal tumor angiogenesis. Future work will include assessment of anti-angiogenic therapy effects using this novel tracer.

ACKNOWLEDGMENT Wim Ceelen is a Senior Clinical Investigator of the Fund for Scientific Research—Flanders (FWO).

REFERENCES

1. Desar IME, van Herpen CML, van Laarhoven HWM, Barentsz JO, Oyen WJG, van der Graaf WTA. Beyond RECIST: molecular and functional imaging techniques for evaluation of response to targeted therapy. *Cancer Treat Rev.* 2009;35:309–321.
2. Kochhar R, Manoharan P, Leahy M, Taylor MB. Imaging in gastrointestinal stromal tumors: current status and future directions. *Clin Radiol.* 2010;65:584–592.
3. Jain RK. Normalization of tumor vasculature: an emerging concept in antiangiogenic therapy. *Science.* 2005;307:58–62.
4. Ceelen W, Smeets P, Backes W, Van Damme N, Boterberg T, Demetter P, et al. Noninvasive monitoring of radiotherapy-induced microvascular changes using dynamic contrast enhanced magnetic resonance imaging (DCE-MRI) in a colorectal tumor model. *Int J Radiat Oncol Biol.* 2006;64:1188–1196.
5. Ceelen W, Boterberg T, Smeets P, Van Damme N, Demetter P, Zwaenepoel O, et al. Recombinant human erythropoietin alpha modulates the effects of radiotherapy on colorectal cancer microvessels. *Br J Cancer.* 2007;96:692–700.
6. Meyer A, Auemheimer J, Modlinger A, Kessler H. Targeting RGD recognizing integrins: Drug development, biomaterial research, tumor imaging and targeting. *Current Pharm Design.* 2006;12:2723–2747.
7. Beer AJ, Schwaiger M. Imaging of integrin alpha v beta 3 expression. *Cancer Metastasis Rev.* 2008;27:631–644.
8. Brooks PC, Clark RAF, Cheresh DA. Requirement of vascular integrin alpha(V)beta(3) for angiogenesis. *Science.* 1994;264:569–571.
9. Debergh I, Van Damme N, Pattyn P, Peeters M, Ceelen WP. The low-molecular-weight heparin, nadroparin, inhibits tumor angiogenesis in a rodent dorsal skinfold chamber model. *Br J Cancer.* 2010;102(5):837–43.
10. Schnell O, Krebs B, Wagner E, Romagna A, Beer AJ, Grau SJ, et al.. Expression of integrin alphavbeta3 in gliomas correlates with tumor grade and is not restricted to tumor vasculature. *Brain Pathol.* 2008; 18(3):378–86.
11. Kiessling F, Morgenstern B, Zhang C. Contrast agents and applications to assess tumor angiogenesis in vivo by magnetic resonance imaging. *Curr Med Chem.* 2007;14:77–91.
12. Marelli UK, Rechenmacher F, Sobahi TRA, Mas-Moruno C, Kessler H. Tumor targeting via integrin ligands. *Front Oncol.* 2013;3:222.
13. Hood J, Cheresh D. Role of integrins in cell invasion and migration. *Nat Rev Cancer.* 2002;2:91–100.
14. Dunehoo A, Anderson M, Majumdar S, Kobayashi N, Berkland C, Siahaan TJ. Cell adhesion molecules for targeting drug delivery. *J Pharm Sci. 2006*;95:1856–1872.
15. Kemperman H, Wijnands YM, Roos E. Alpha V integrins on HT-29 colon carcinoma cells: adhesion to fibronectin is mediated solely by small amounts of alpha V beta 6, and alpha V beta 5 is codistributed with actin fibers. *Exp Cell Res.* 1997;234:156–164.
16. Haier J, Nasralla M, Nicolson GL. Different adhesion properties of highly and poorly metastatic HT-29 colon carcinoma cells with extracellular matrix components: role of integrin expression and cytoskeletal components. *Br J Cancer.* 1999;80:1867–1874.
17. Liu Z, Jia B, Shi J, Jin X, Zhao H, Li F, et al. Tumor uptake of the RGD dimeric probe (99m)Tc-G(3)-2P(4)-RGD2 is correlated with integrin alpha(v)beta(3) expressed on both tumor cells and neovasculature. *Bioconjug Chem.* 2010;21(3):548–555.
18. Zhou Y, Kim YS, Chakraborty S, Shi J, Gao H, Liu S. 99mTc-labeled cyclic RGD peptides for noninvasive monitoring of tumor integrin αVβ3 expression. *Mol Imaging.* 2011;10:386–397.
19. Winter PM, Caruthers SD, Kassner A, Harris TD, Chinen LK, Allen JS, et al. Molecular imaging of angiogenesis in nascent vx-2 rabbit tumors using a novel alpha(v)beta(3)-targeted nanoparticle and 1.5 tesla magnetic resonance imaging. *Cancer Res.* 2003;63:5838–5843.
20. Mulder WJ, Strijkers GJ, Habets JW, Bleeker EJ, van der Schaft DW, Storm G, et al. MR molecular imaging and fluorescence microscopy for identification of activated tumor endothelium using a bimodal lipidic nanoparticle. *FASEB J.* 2005;19:2008–2010.
21. Zhang C, Jugold M, Woenne EC, Lammers T, Morgenstern B, Mueller MM, et al. Specific targeting of tumor angiogenesis by

RGD-conjugated ultrasmall superparamagnetic iron oxide particles using a clinical 1.5-T magnetic resonance scanner. *Cancer Res*. 2007;67:1555–1562.
22. Jiang T, Zhang CF, Zheng X, Xu XF, Xie X, Liu HC, et al. Noninvasively characterizing the different alpha v beta 3 expression patterns in lung cancers with RgD-USPIO using a clinical 3.0T MR scanner. *Int J Nanomed*. 2009;4:241–249.
23. Kiessling F, Huppert J, Zhang C, Jayapaul J, Zwick S, Woenne EC, et al. RGD-labeled USPIO inhibits adhesion and endocytotic activity of alpha(v)beta(3)-integrin-expressing glioma cells and only accumulates in the vascular tumor compartment. *Radiology*. 2009;253:462–469.
24. Wong C, Stylianopoulos T, Cui J, Martin J, Chauhan VP, Jiang W, et al. Multistage nanoparticle delivery system for deep penetration into tumor tissue. *Proc Natl Acad Sci USA*. 2011;108:2426–2431.
25. Sharma R, Saini S, Ros PR, Hahn PF, Small WC, de Lange EE, et al. Safety profile of ultrasmall superparamagnetic iron oxide ferumoxtran-10: phase II clinical trial data. *J Magn Reson Imaging*. 1999;9:291–294.
26. Sipkins DA, Cheresh DA, Kazemi MR, Nevin LM, Bednarski MD, Li KC. Detection of tumor angiogenesis in vivo by alphaVbeta3-targeted magnetic resonance imaging. *Nat Med.* 1998;4:623–626.
27. Bloch S, Xu B, Ye Y, Liang K, Achilefu S. Internalization of RGD peptide conjugates of near-infrared fluorescent probes in different cell lines occurs via different integrin receptor subtypes. *Proc SPIE.* 2006;6097:60970H.
28. Janssen ML, Oyen WJ, Dijkgraaf I, Massuger LF, Frielink C, Edwards DS, et al. Tumor targeting with radiolabeled alpha(v)-beta(3) integrin binding peptides in a nude mouse model. *Cancer Res*. 2002;62(21):6146–51.
29. Dijkgraaf I, Kruijtzer JA, Liu S, Soede AC, Oyen WJ, Corstens FH, et al. Improved targeting of the alpha(v)beta (3) integrin by multimerisation of RGD peptides. *Eur J Nucl Med Mol Imaging*. 2007;34(2):267–73.
30. Strijkers GJ, Kluza E, Van Tilborg GAF, van der Schaft DWJ, Griffioen AW, Mulder WJM, et al. Paramagnetic and fluorescent liposomes for target-specific imaging and therapy of tumor angiogenesis. *Angiogenesis*. 2010;13:161–173.
31. Avraamides CJ, Garmy-Susini B, Varner JA. Integrins in angiogenesis and lymphangiogenesis. *Nat Rev Cancer.* 2008;8:604–617.